The Effect of Cladding Layer Thickness on Large Optical Cavity 650-nm Lasers

Peter M. Smowton, John D. Thomson, M. Yin, Susan V. Dewar, Peter Blood, A. Catrina Bryce, John H. Marsh, C. J. Hamilton, and C. C. Button

***Abstract*—The reduction in penetration of the optical mode into the cladding layers in large optical cavity (LOC) laser structures offers the possibility of reducing the cladding-layer thickness. This could be particularly beneficial in GaInP–AlGaInP high-power devices by reducing the thermal impedance and the electrical series resistance. We have designed and characterized 650-nm LOC lasers by modeling the optical loss due to incomplete confinement of the optical mode by the cladding layers and calculating the thermally activated leakage current. This indicated that the cladding thickness could be reduced to 0.5 μm without adversely affecting performance. We investigated devices with 0.3-, 0.5-, and 1-μm-wide cladding layers. The measured optical mode loss of the 0.3 -μm-wide cladding device was 36.2 cm^{-1} compared with 12.4 and 11.3 cm^{-1} for the 0.5- and 1 -μm-wide cladding samples, respectively. The threshold current densities of the 0.5- and 1.0-μm devices were similar over the temperature range investigated (120–320 K), whereas the 0.3 -μm devices had significantly higher threshold current density. We show that this can be attributed to the higher optical loss and increased leakage current through the thin cladding layer. The intrinsic gain characteristics were the same in all the devices, irrespective of the cladding-layer thickness. The measured thermal impedance of 2-mm-long devices was reduced from 30.7 to 22.3 K/W by reducing the cladding thickness from 1 to 0.5 μm. Our results show that this can be achieved without detriment to the threshold characteristics.**

I. Introduction

GaInP–AlGaInP high-power lasers operating in the wavelength range of 630–690 nm are required for a number of applications, including photodynamic therapy and read/write optical storage systems. Unfortunately p-doped AlGaInP has a large electrical resistivity due to incomplete activation of the dopant [1], low hole mobility [2], and a relatively poor thermal conductivity [3]. These properties exacerbate the thermal management problems associated with high power lasers. However, the reduction in penetration of the optical mode into the cladding layers which occurs in large optical cavity (LOC) structures [4] opens up the possibility of reducing the cladding-layer thickness, thereby reducing the electrical and thermal resistance. In addition to the need to maintain coupling of the optical mode to the quantum wells, there are two further factors which limit the extent to which the cladding thickness can be reduced. The first is the leakage of the mode into the absorbing GaAs contact layer and substrate, increasing the gain requirement and hence the intrinsic threshold current. The second is the thermally activated leakage current, which in GaInP-based lasers is due to drift and diffusion of electrons through the p-cladding layer. The leakage current increases as the cladding thickness is reduced, increasing the threshold current, which could cause an increase in power dissipation and increased internal temperature rise, negating the benefits of the reduced thermal impedance. In this paper, we investigate the interplay of these effects by analyzing the performance of LOC structures with three different values of cladding-layer thickness 0.3, 0.5, and 1 μm.

We begin by describing, in Section II, the design of the laser devices, including calculations of the effect of reduced cladding-layer thickness on optical mode loss and thermally activated leakage current. In Section III, we describe results of measurements of threshold current, optical mode loss, optical gain, and thermal impedance of devices with 0.3 -, 0.5-, and 1 -μm cladding thickness. These results show that a reduction in thermal impedance can be achieved with a cladding thickness of 0.5 μm. However, although further reduction probably occurs for a thickness of 0.3 μm, the threshold current of these devices is greatly increased due to increased optical mode loss and increased leakage current.

II. Laser Design

The active region of the devices consisted of three 45 -Å wide, compressively strained, $Ga_{0.42}In_{0.58}P$ quantum wells separated by 80 Å of $(Al_{0.35}Ga_{0.65})_{0.52}In_{0.48}P$ and designed to emit at 650 nm. The rest of the waveguide core was also $(Al_{0.35}Ga_{0.65})_{0.52}In_{0.48}P$, and this was clad with layers of $(Al_{0.7}Ga_{0.3})_{0.52}In_{0.48}P$ nominally doped $5 \times 10^{17} cm^{-3}$ using Zn on the p-side and with $1 \times 10^{18} cm^{-3}$ Si on the n-side. These layers were grown by MOCVD on a misorientated E–J GaAs substrate tilted 10° off the (100) toward [111] A to produce disordered material.

The aim in designing a LOC structure is to spread the mode by using a wide waveguide core. Since the second guided mode is not coupled to the active region, the upper limit to the width of the core is set by the onset of the third mode. The laser structure was assumed to be infinite in the lateral and longitudinal directions, resulting in a vertical multilayer slab waveguide problem.

Manuscript received August 14, 2001. This work was supported by the U.K. Engineering and Physical Sciences Research Council under Grant GR/L94000/01.

P. M. Smowton, J. D. Thomson, S. V. Dewar, and P. Blood are with the Department of Physics and Astronomy, Cardiff University, Cardiff CF24 3YB, U.K.

M. Yin was with the Department of Physics and Astronomy, Cardiff University, Cardiff, CF24 3YB, U.K. He is now with the Electronic Engineering Laboratory, University of Kent at Canterbury, Canterbury, Kent CT2 7NT, U.K.

A. C. Bryce and J. H. Marsh are with the Department of Electronic and Electrical Engineering, University of Glasgow, Glasgow GL12 8LT, U.K.

C. J. Hamilton was with the Department of Electronic and Electrical Engineering, University of Glasgow, Rankine Building, Glasgow, GL12 8LT, U.K. He is now with Intense Photonics, Kelvin Campus, West of Scotland Science Park, Glasgow G20 0TH, U.K.

C. C. Button was with the Department of Electronic and Electrical Engineering, University of Sheffield, Sheffield S1 3JD, U.K. He is now with Marconi Caswell Ltd., Northhamptonshire NN12 8EQ, U.K.

Publisher Item Identifier S 0018-9197(02)01752-9.

TABLE I
CALCULATED VALUES OF THE ATTENUATION COEFFICIENT FOR STRUCTURES WITH DIFFERENT CLADDING LAYER THICKNESS

Cladding layer thickness / μm	Loss / cm mode 1
0.3	17.8
0.5	0.7
1.0	0.0003

The refractive indices of the AlGaInP layers were taken from [5] and those for GaAs from [6]. Using the transfer matrix method, a total core width of 6300 Å was determined by increasing the width until a third guided mode appeared and then reducing the width by 10% to allow for unintended variation in the width of the as-grown layers.

Our aim was to reduce the cladding-layer thickness while avoiding leakage of the mode into the absorbing, high index GaAs p-contact layer and n-GaAs substrate. We calculated the loss by the transfer matrix approach, assuming that the outer GaAs layers were infinitely thick with a complex refractive index taking account of the absorption of the material. The remaining layers were assumed to be loss-free. The calculation did not take account of other sources of optical loss such as interface scattering since these should be the same for different cladding thicknesses. We calculated the attenuation coefficient of the mode intensity for cladding-layer thicknesses of 0.3, 0.5 , and 1.0 μm. The second guided mode, being the asymmetric solution, had negligible overlap with the gain region, and we therefore concentrated on the loss values for the first mode, given in Table I, which show a significant increase in loss from 0.0003 to 17.8 cm^{-1}, going from the thick to thin cladding layer.

The calculated values are the loss due to incomplete confinement of the optical mode and in a real device there is additional loss due to scattering and free carrier absorption. To assess the significance of the values in Table I, we compared them with the loss in a typical GaInP–AlGaInP laser with normal cladding thickness. This loss is made up of the mirror loss and the internal optical mode loss, α_i. For these devices, values of α_i are typically in the range 3–15 cm^{-1} (e.g., [7]). Therefore, for a 550 -μm-long device, the loss is typically $\approx$30 cm^{-1} (mirror loss $\approx$22 cm^{-1} and $\alpha_i = 8$ cm^{-1}). The loss due to mode leakage (Table I) for the 0.5- and 1-μm-thick cladding samples are negligible compared with this value, but the 0.3-μm sample incurs a significant extra loss of 17.8 cm^{-1}. The value of α_i may be lower in LOC structures than the typical value above due to reduced overlap of the optical mode with the doped cladding layers [4]. Except for very long devices, the distributed mirror loss is greater than α_i, and we conclude that the cladding-layer thickness can be reduced to 0.5 μm without incurring significant addition mode loss, but when the thickness is reduced to 0.3 μm, the total loss may increase by about 50%.

We next consider the increase in thermally activated loss of electrons through the p-cladding layer as the cladding thickness is reduced. This leakage current can be significant for GaInP–AlGaInP devices, particularly at high temperatures or for short emission wavelengths [8], [9]. The leakage current density through the p-cladding layer J_L depends upon the thickness of the cladding layer w_c, according to the expression

TABLE II
MATERIAL PARAMETERS $(Al_{0.7}Ga_{0.3})In_{0.51}P_{0.49}$ USED IN THE LEAKAGE CALCULATION

SYMBOL	PARAMETER	VALUE	UNITS
D_n	Electron diffusion coefficient	4.39	cm^2/s
T	Temperature	300	K
m_e	Density of states (X) electron mass	0.6	m_o
E_g	Bandgap (X)	2.26	eV
m_h	Density of states hole mass	0.35	m_o
L_n	Minority carrier diffusion length	0.3	μm
μ_e	Minority carrier mobility	160	cm^{2}V^{-1}s^{-1}
τ_{cnr}	non-radiative lifetime	2×10^{-10}	s
P	Ionised dopant concentration	5×10^{17}	cm^{-3}
μ_h	Majority carrier mobility	7	cm^{2}V^{-1}s^{-1}

[8], [9]

$$J_L = eD_n 2\left(\frac{m^*_{cn}kT}{2\pi\hbar}\right)^{3/2}\exp\left(\frac{E_{fe}-E_c}{kT}\right) \cdot\left\{\left(\frac{1}{L_n^2}+\frac{1}{4z^2}\right)^{1/2}\coth\left(\left(\frac{1}{L_n^2}+\frac{1}{4z^2}\right)^{1/2}w_c\right)+\frac{1}{2z}\right\}$$

where

- e electronic charge;
- D_n minority electron diffusion coefficient;
- m_{cn} electron mass in the cladding layer;
- k Boltzmann constant;
- T temperature;
- $\hbar$ Planck constant divided by 2π;
- E_{fe} energy of the electron quasi-Fermi level;
- E_c energy of the lowest conduction band edge in the cladding layer;
- L_n diffusion length;
- z length characteristic of drift leakage, which is a function of the total hole current flowing through the p-cladding layer J_h, ($z = kTp\mu_h/J_h$, where p is the activated dopant concentration and μ_h the majority carrier mobility).

We calculated the leakage current as a function of cladding-layer thickness w_c for a fixed optical loss, i.e., the same quasi-Fermi level separation and radiative current density. The values of material parameters used [9], [10] are given in Table II. As illustrated in the inset of Fig. 1, the energy step $(E_{fe} - E_c)$ is given by $(E_x - \Delta E_f - \Delta E_{vp})$, where E_x is the smallest (X) band gap in the cladding layer and ΔE_{vp} is the difference between the valence band edge and the hole Fermi level in the p-cladding layer $[=kT\ln(N_v/p)]$, where N_v is the effective density of states in the valence band [11]. Calculated values of leakage current at 300 K are shown in Fig. 1 for two different quasi-Fermi level separations of 1.910 and 1.922 eV. From the experimental data presented in Section III-C, these values correspond to optical losses of about 18 and 33 cm^{-1} in our structures (Fig. 5).

The results in Fig. 1 show that, for both values of optical loss, the leakage current remains constant down to a cladding-layer thickness of about 0.5 μm, then increases rapidly below about 0.3 μm. However, any increase in optical loss due to a reduction in cladding-layer thickness increases the quasi-Fermi level separation, increasing the leakage current more dramatically than

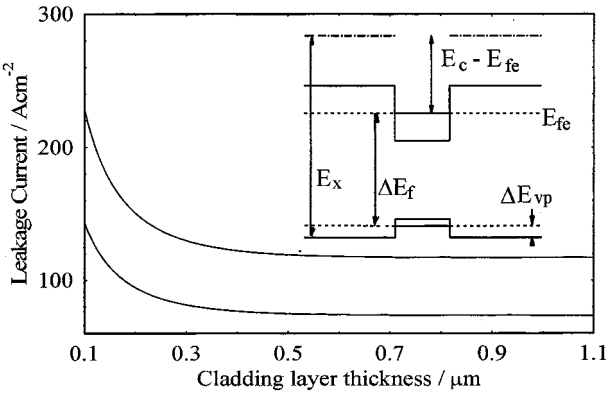

Fig. 1. Calculated leakage current versus cladding-layer thickness at 300 K for a GaInP laser structure. The material parameters are given in Table I and the curves correspond to $\Delta E_f = 1.910$ (lower curve) and 1.922 eV (upper curve). The inset is a schematic representation of the band structure to illustrate the determination of $E_{fe} - E_c$ from the available data for E_x, and ΔE_{vp} and the input value of ΔE_f.

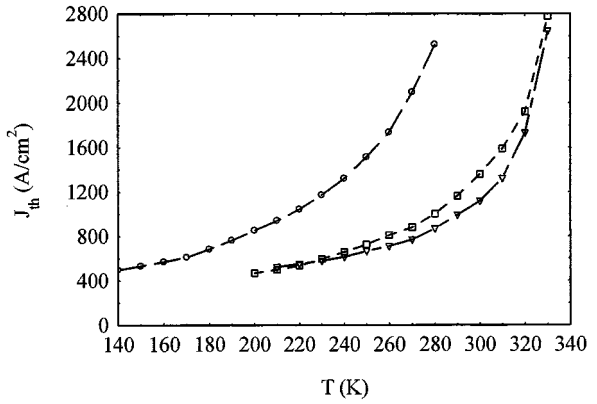

Fig. 2. Threshold current density versus temperature for 500-μm-long devices with cladding-layer thicknesses of 0.3-μm (circles), 0.5 -μm (squares), and 1.0-μm-wide (triangles) cladding-layers thickness.

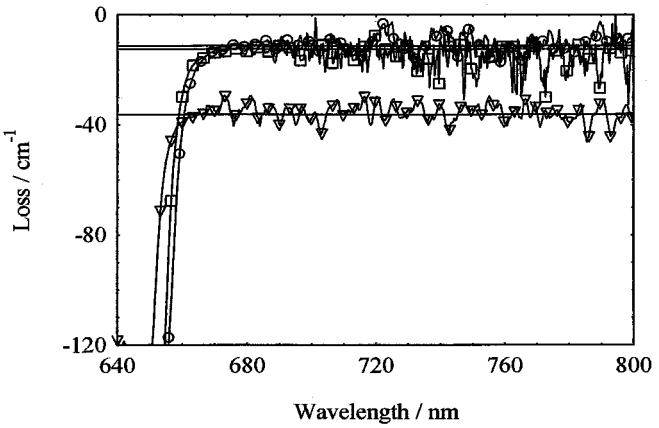

Fig. 3. Optical loss measured using the single pass multisection device method for samples with cladding layers of 0.3 μm (triangles), 0.5 μm (squares), and 1.0 μm (circles). The values of α_i derived from the measurements are represented by the wavelength-independent (solid lines).

suggested by this figure. This is one of the factors to be explored in the experimental evaluation of the devices.

The sensitivity of the leakage current to the cladding thickness is dependent on the quality of the material. It is clear from (1) that the leakage current is a sensitive function of cladding thickness when the diffusion length L_n is less than twice the drift length z and when L_n is comparable to the cladding thickness w_c. A larger sensitivity than we calculated in Fig. 1 would be apparent if the material was improved so that z and L_n were both increased. However, the calculations suggest that for our material the cladding layer can be reduced to 0.5 μm without a significant increase in leakage current. We estimate that a further reduction in thickness to 0.3 μm would lead to an increase of leakage current causing an increase in threshold current of about 10% beyond that expected due to the increase in optical losses alone.

Overall, the calculations predict that the cladding thickness can be reduced to about 0.5 μm without significant change in optical loss and carrier leakage. In the following section, we present an analysis of the performance of devices with cladding-layer thicknesses of 1.0 , 0.5 , and 0.3 μm. The material was fabricated into 75-μm-wide oxide isolated stripe devices and also into multisection devices [12] for measurement of optical gain, optical loss, and quasi-Fermi level separation. The lasers were operated pulsed using a 300–ns-wide pulse with a duty cycle of 0.03%. The expected operation of the LOC structures was confirmed by measuring the vertical far-field pattern and comparing it with the calculations.

III. Experimental Results

A. Threshold Current

Measurements of the threshold current density versus temperature for devices with a 500-μm-long cavity length are plotted in Fig. 2. The threshold current density of the 0.3-μm cladding device is significantly higher than that of the other devices at all temperatures. At low temperatures the threshold current increases linearly with temperature, characteristic of the intrinsic radiative current in the quantum well [7], [9] and the threshold current density in this region is higher for the 0.3-μm cladding-layer device because of the higher optical loss. The thermally activated leakage current develops at lower temperature than in the wider cladding devices [7], [9] because the larger quasi Fermi-level separation exacerbates the leakage current. The 0.3-μm cladding devices did not lase at room temperature. This behavior is broadly as predicted in Section II. The leakage current is discussed in more detail in Section III-C.

B. Optical Loss

Measurements of the optical loss through passive material were made using the single pass, multisection stripe length method [12] and the results are plotted as a function of wavelength in Fig. 3. At short wavelengths the total loss consists of modal absorption due to valence band to conduction band transitions and internal optical mode loss and the onset of this strong absorption indicates the absorption edge of the quantum well structure. Although the three structures were grown sequentially, the absorption edge—and indeed the exciton peaks as measured using edge photovoltage absorption spectroscopy [7]—are at slightly different energies. The differences in the absorption edge of 14.4 meV (0.3–1.0 μm), and 3.7 meV (0.5–1.0 μm) are small and could be due to, for example, a well width difference of two monolayers and less than one monolayer, respectively.

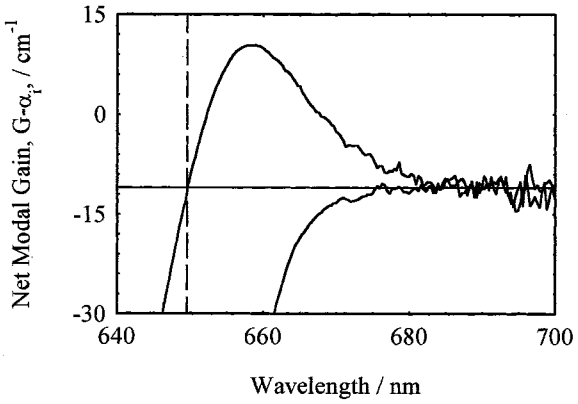

Fig. 4. Example of determination of quasi-Fermi level separation using independently measured loss and gain spectra. At long wavelengths beyond the band edge, there is no absorption or optical gain due to the quantum-well structure and the "net gain" in both cases corresponds to the modal loss. The quasi-Fermi level separation is obtained from the transparency point, which is the photon energy where the gain is equal to the losses, as indicated by the intersection of the horizontal line, corresponding to the loss, with the gain spectrum.

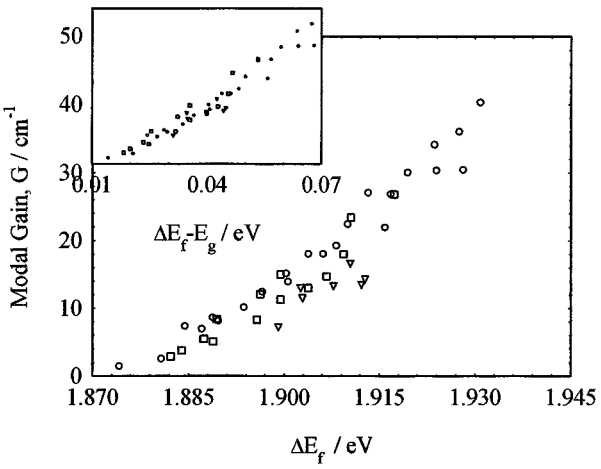

Fig. 5. Experimental data for peak modal gain versus quasi-Fermi level separation for samples with cladding layers of 0.3 μm (triangles), 0.5 μm (squares), and 1.0 μm (circles). The inset shows the data re-plotted relative to the energy of the band edge to take account of small difference in band edge energy between the samples.

At long wavelengths, below the band edge, the measurement yields a value of the internal optical mode loss. The values for the 0.5 - and 1-μm-wide cladding layers are very similar (12.4 ± 3.7 and 11.3 ± 1.9 cm^{-1}, respectively), whereas the 0.3-μm-wide cladding sample has a significantly higher value of 36.2 ± 6.9 cm^{-1}. These measurements include both the loss due to optical leakage through the p-cladding calculated in Section II and other sources of loss, such as the scattering loss. The measured data are consistent with the calculated values in Table I and loss due to other sources of about 11 cm^{-1}. The measured loss of 36 cm^{-1} for the 0.3-μm-wide cladding layer is large compared to the mirror loss of 24 cm^{-1} for a typical uncoated 500-μm-long device.

C. Gain, Quasi-Fermi Level Separation, and Leakage Current

We measured the modal gain as a function of quasi-Fermi level separation in electrically pumped material using the single-pass multisection device method [12]. These data enable us to confirm that the intrinsic properties of the active regions of all the devices are indeed the same and allow us to determine the quasi-Fermi level separation from the measured values of loss and, hence, compute the leakage currents from (1).

To illustrate the determination of the quasi-Fermi level separation, the (passive) optical loss spectrum for the 1.0-μm structure, as shown in Fig. 3, is plotted in Fig. 4 together with the net optical gain spectrum (G–α_i) measured with a pump current density of 1200 A·cm^{-2}. At long wavelengths, above the band edge, there is no optical gain and both measurements give the optical mode loss α_i. If we assume that α_i is independent of wavelength, we can extrapolate the value of α_i to short wavelengths, as shown in Fig. 4, and determine the quasi-Fermi level separation from the energy at which the net gain $= \alpha_i$ corresponding to the transparency point. The loss data between 680 and 800 nm shown in Fig. 3 demonstrates that α_i is independent of wavelength over this narrower range and supports the assumption made.

Net gain (G–α_i) spectra were measured as a function of drive current at a temperature of 300 K and values of G at the peak of the spectrum (obtained by adding the measured value of α_i) and quasi-Fermi level separation ΔE_f were derived. Fig. 5 is a plot of the peak value of G for each current versus the corresponding quasi-Fermi level separation ΔE_f. The inset of Fig. 5 shows the same data plotted as a function of $(\Delta E_f - E_g)$, where E_g is the transition energy of the quantum well, to remove the effect of the small differences in absorption edge energy of different samples, shown in Fig. 3. The data of Fig. 5 confirm that the intrinsic relation between gain and relative quasi-Fermi level separation is the same for all the active regions, irrespective of the cladding-layer thickness, as we would expect.

Since we have measured the optical mode loss and can calculate the mirror loss for a given device length, these data allows us to determine the quasi-Fermi level separation at threshold for each cladding-layer thicknesses. The 0.3-μm cladding has a large optical mode loss and the quasi-Fermi level separation was obtained by extrapolating the plot in Fig. 5. We then used (1) to calculate the leakage current expected for each device at 300 K. We used the material parameters listed in Table II except that we used a p-doping level of 1×10^{17}cm^{-3} as measured for these samples [13]. The recombination current in the quantum well, required for the calculation of leakage current, was estimated by linearly extrapolating the low temperature data in Fig. 2 to 300 K. Results for the leakage current are shown in Table III for a cavity length of 500 μm, together with estimates obtained from the experimental data by subtracting the extrapolated value at 300 K from the measured value. Note that the "calculated" values are obtained from (1) using *experimentally determined* values for the optical mode loss and the relation between gain and quasi-Fermi level separation. These calculated data and the threshold current results confirm there is little increase in leakage when the cladding thickness is decreased to 0.5 μm. However, the calculations show that the leakage current is about 2500 A·cm^{-2} for a cladding thickness of 0.3 μm, due primarily to the higher electron quasi Fermi level. Linearly extrapolating the low-temperature data for this sample in Fig. 2 suggests the threshold current due to recombination in the well itself at room temperature is about 1000 A·cm^{-2}, giving

TABLE III
LEAKAGE CURRENT VALUES AT ROOM TEMPERATURE CALCULATED USING (1) WITH EXPERIMENTAL DATA FOR THE QUASI-FERMI LEVEL SEPARATION DETERMINED FROM THE MEASURED OPTICAL LOSS. LEAKAGE CURRENT VALUES ESTIMATED FROM THE MEASURED THRESHOLD CURRENT DATA IN FIG. 2 ARE SHOWN FOR COMPARISON

0.5 mm cavity	Optical Loss (cm^{-1})	ΔE_f (eV)	Calculated Leakage Current (Acm^{-2})	Estimated Leakage Current (Acm^{-2})
1.0 μm	33.3	1.922	424	400
0.5 μm	34.4	1.924	458	610
0.3 μm	58.2	1.960	2500	-

a total threshold current of about 3500 $A{\cdot}cm^{-2}$, which is indeed greater than the drive capability of our apparatus. We conclude that the cladding thickness can be reduced to about 0.5 μm without any significant increase in the thermally activated leakage current at room temperature.

D. Thermal Impedance Measurements

For satisfactory high power performance, it is essential that the heat generated within the device is efficiently removed to the heat sink, and this is usually quantified by the thermal impedance. In GaInP–AlGaInP structures, the AlGaInP layers suffer from poor electrical and thermal conduction, which leads to increased generation and inefficient removal of heat from the active region. The resulting increase in operating temperature can cause an increase in the threshold current density, a reduction of output power, a shift to longer wavelengths, and poor reliability. To measure the thermal impedance, we operated our laser devices at a heatsink temperature of 200 K at a pulse width of 300 ns and a repetition rate of 1 kHz. By increasing the pulse length, we confirmed that the increase in the temperature of the active region due to the 300- ns pulse was negligible. The pulse was superimposed on a CW drive current and the temperature rise of the active region (dT_{ar}) was measured from the change of laser wavelength as the CW drive current was increased $(d\lambda_l)$. The amplitude of the pulse was reduced as the CW current was increased to maintain the total current at $1.1 \times I_{\rm th}$, where $I_{\rm th}$ is the threshold current. The electrical input power $(P_{\rm CW})$ was derived from the measured CW drive current and voltage. The wavelength change was calibrated by measuring the laser wavelength change with heatsink temperature $d\lambda_l/dT$ over the temperature range 200–300 K. The value of $d\lambda_l/dT$ was 0.150 $\pm$ 0.004 nm/K for both the 1.0- and 0.5-μm-thick cladding-layer structures, which is consistent with the band gap change with temperature [9]. The thermal impedance was then obtained from the following relation:

$$R_{\rm th} = \frac{dT_{ar}}{dP_{\rm CW}} = \frac{dT_{ar}}{d\lambda_l}\,\frac{d\lambda_l}{dP_{\rm CW}}.$$

The temperature rise as a function of the input power for the 0.5- and 1-μm-wide cladding-layer samples of length 2000 μm is shown in Fig. 6. The plot is linear in both cases, as it is for all the structures examined; the small deviations from the straight line occur presumably because of the discontinuous change in laser wavelength with temperature due to mode jumps. From such data, we deduced values of thermal impedance of (30.7 $\pm$ 1.4) K/W and (22.3 $\pm$ 0.6) K/W for the 1- and 0.5-μm-wide

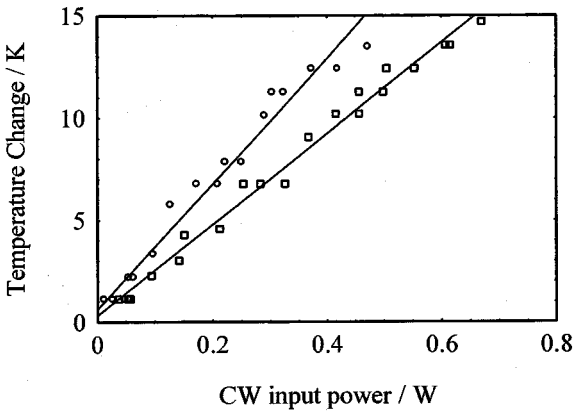

Fig. 6. Experimental results for the temperature increase of the active region of devices with 1.0- (circles) and 0.5-μm (squares) thick cladding layers as a function of input power, for a heat-sink temperature of 200 K.

cladding-layer samples of length 2000 μm and values of (47.7 $\pm$ 1.5) K/W and (36.1 $\pm$ 1.7) K/W for the 1- and 0.5-μm-wide cladding-layer samples 750 μm in length. Similar results were obtained at a heat-sink temperature of 250 K.

The way that the thermal impedance varies with device length and thickness depends upon the location of the sources of heat and the form of heat flow within the device. For devices mounted active-side up, the thermal impedance is expected to be proportional to $(1/L)\ln(t)$, whereas it is proportional to $1/(tL)$ for the ideal 1-D heat flow approximated in an active-side-down mounting [14], where t is the thickness of material and L is the device length. The variation with device length is as expected for devices mounted active-side uppermost. The results for devices with 1-μm-wide cladding layers are of the same order as previously reported values of thermal impedance for AlGaInP-based lasers (e.g., [14], [15]). These results demonstrate that there is a measurable reduction in the thermal impedance of devices going from a cladding-layer thickness of 1–0.5 μm in thickness, so devices with 0.5-μm-wide cladding layers should have significant performance advantages for high-power lasers.

IV. SUMMARY

We have designed and evaluated the performance of large optical cavity 650 -nm GaInP laser diodes in which the cladding-layer thickness was reduced from 1 to 0.5 μm and 0.3 μm. The experimental results show that the thermal impedance is reduced with this reduction in cladding thickness, and for the 1.0- and 0.5-μm cladding devices, there is no increase in the optical mode loss and thermally induced carrier leakage. However, for the 0.3-μm cladding-layer thickness, the optical mode penetrates sufficiently into the GaAs contact and substrate that the mode loss increases substantially such that the devices do not lase at room temperature. The measured changes in mode loss are in agreement with calculations, and the threshold current behavior agrees with values of leakage calculated from measured mode loss and quasi-Fermi level separations. Measurements of gain spectra show that the intrinsic relation between the gain and the quasi-Fermi level separation is the same for all structures as expected. This work indicates that improvements in the high-power performance of a red-emitting laser can be obtained

by using a LOC structure with cladding thickness reduced to about 0.5 μm.

REFERENCES

[1] Y. Ohba, Y. Nishikawa, C. Nozaki, and T. Nakanisi, "A study of p-type doping for AlGaInP grown by low pressure MOCVD," *J. Cryst. Growth*, vol. 93, pp. 613–617, 1988.

[2] Y. Ohba, Y. Ishikawa, H. Sugawara, M. Yamamoto, and T. Nakanisi, "Growth of high quality InGaInP epilayers by MOCVD using Methyl metalorganics and their application to visible semiconductor lasers," *J. Cryst. Growth*, vol. 77, pp. 374–379, 1986.

[3] H. Fujii, Y. Ueno, and K. Endo, "Effect of thermal resistivity on the catastrophic optical damage power density of AlGaInP laser diodes," *Appl. Phys. Lett.*, vol. 62, pp. 2114–2116, 1993.

[4] N. Lichtenstein, R. Winterhoff, F. Scholz, H. Schweizer, S. Weiss, M. Hutter, and H. Reichl, "The impact of LOC Structures on 670nm (Al)GaInP High Power Lasers," *IEEE J. Select. Topics Quantum Electron.*, vol. 6, pp. 564–570, 2000.

[5] Y. Kaneko and K. Kishino, "Refractive Indices measurement of $(GaInP)_m/(AlInP)_n$ quasiquarternaries and GaInP/AlInP multiple quantum wells," *J. Appl. Phys.*, vol. 76, pp. 1809–1818, 1994.

[6] M. A. Afromowitz, "Refractive index of $Ga_{1-x}Al_xAs$," *Solid State Commun.*, vol. 15, pp. 59–63, 1974.

[7] P. M. Smowton, P. Blood, P. C. Mogensen, and D. P. Bour, "Role of sublinear gain-current relationship in compressive and tensile strained 630 nm GaInP lasers," *Int. J. Optoelectron.*, vol. 10, pp. 383–391, 1996.

[8] D. P. Bour, D. W. Treat, R. L. Thornton, R. S. Geels, and D. F. Welch, "Drift leakage current in AlGaInP quantum well lasers," *IEEE J. Quantum Electron.*, vol. 29, pp. 1337–1343, 1993.

[9] P. M. Smowton and P. Blood, "Visible emitting (AlGa)InP laser diodes," in *Strained Layer Quantum Wells and Their Applications*, M. O. Manasreh, Ed. London, U.K.: Gordon and Breach, 1997.

[10] S. A. Wood, C. H. Molloy, P. M. Smowton, P. Blood, and C. C. Button, "Minority carrier effects in GaInP laser diodes," *IEEE J. Quantum Electron.*, vol. 36, pp. 742–750, 2000.

[11] P. M. Smowton and P. Blood, "GaInP–(Al_yGa_{1-y})InP 670nm quantum well lasers for high temperature operation," *IEEE J. Quantum Electron.*, vol. 31, pp. 2159–2164, 1995.

[12] J. D. Thomson, H. D. Summers, P. J. Hulyer, P. M. Smowton, and P. Blood, "Determination of single-pass optical gain and internal loss using a multisection device," *Appl. Phys. Lett.*, vol. 75, pp. 2527–2529, 1999.

[13] M. Yin, P. M. Smowton, P. Blood, B. McAuley, and C. C. Button, "S-shaped negative differential resistance in 650 nm quantum well laser diodes," *Solid State Electron.*, pp. 447–452, 2000.

[14] O. J. F. Martin, G-L. Bona, and P. Wolf, "Thermal behavior of visible AlGaInP–GaInP ridge laser diodes," *IEEE J. Quantum Electron.*, vol. 28, pp. 2582–2588, 1992.

[15] H. Okuda, M. Ishikawa, H. Shiozawa, Y. Watanabe, K. Itaya, K. Nitta, G-I. Hatakoshi, Y. Kokubun, and Y. Uematsu, "Highly reliable InGaP/InGaAlP visible light emitting inner stripe lasers with 667nm lasing wavelength," *IEEE J. Quantum Electron.*, vol. 25, pp. 1477–1482, 1989.

Peter M. Smowton received the B.Sc. degree in physics and electronics in 1987 and the and the Ph.D. degree in electrical engineering from University of Wales, Cardiff, U.K., in 1991, where he studied the frequency stabilization of laser diodes.

During 1991-1992, he was responsible for device processing at Cardiff Microelectronics Center. He has been involved in the design and characterization of strained-layer (AlGa)InP laser diodes. Currently, he is a Lecturer in semiconductor optoelectronics in the Department of Physics and Astronomy, Cardiff University. His topics of research include quantum-dot lasers, high-power red lasers for photodynamic therapy, and the physics of InGaN light-emitting devices.

Dr. Smowton is a member of the IEEE LEOS Society and the Institute of Physics (London, U.K.).

John D. Thomson received the M.Sci. degree in physics from the University of St. Andrews, St. Andrews, U.K., in 1997, and the Ph.D. degree in physics from Cardiff University, Cardiff, Wales, U.K., in 2001. His doctoral research was on optical gain studies of quantum-confined structures.

He is a Research Associate with the Optoelectronics Research Group, Cardiff University, where he has been involved in the research of red emitting lasers and quantum-dot structures. He is currently working on GaN light-emitting devices.

Dr. Thomson is a member of the Institute of Physics (London, U.K.).

M. Yin, photograph and biography not available at the time of publication.

Susan V. Dewar received the B.Sc. degree in physics and astronomy from University College London, London, U.K., in 1984, and the Ph.D. degree from the Department of Electronic and Electrical Engineering, University of Sheffield, Sheffield, U.K., in 1991.

Since 1991, she has been a Lecturer in the Department of Physics and Astronomy, Cardiff University, Cardiff, Wales, U.K. Her research interests include the theoretical and numerical modeling of semiconductor optoelectronic devices.

Peter Blood is Professor of Physics in Cardiff University, Cardiff, Wales, U.K., where he also leads a research group in optoelectronics. He is also Director of the Cardiff Centre for Multidisciplinary Microtechnology, a Centre of Excellence supported by the Welsh Development Agency. He was previously with Philips Research Laboratories, Redhill, U.K. His current research interests include quantum wells and quantum dots, wide-gap nitrides, and experimental studies of optical gain and spontaneous emission. He has co-authored two books on electrical characterization of semiconductors and gives short courses at major international conferences.

A. Catrina Bryce (M'91–SM'99) was born in Glasgow, Scotland, U.K., in 1956. She received the B.Sc. degree in physics from Glasgow University, Glasgow, Scotland, U.K., in 1978, the M.Sc. degree in amorphous materials from Dundee University, Scotland, U.K., in 1979, and the Ph.D. degree in phonon scattering in thin-film glasses from Glasgow University.

In 1985, she joined the Department of Electronics and Electrical Engineering, University of Glasgow, as a Research Assistant, working in molecular beam epitaxy. In 1987, she joined the Optoelectronics Group to work on nonlinear optical properties of GaInAs quantum-well structures at 1.5 mm. Since then, her research has included GaInAs–InP electrooptic modulators, quantum-well intermixing (particularly in 1.55-mm and 980-nm material systems), lasers at 980 nm and 1.55 mm, optoelectronic integration, and III–V semiconductor lasers.

John H. Marsh (M'91–SM'91–F'00) is the Chief Research Officer of Intense Photonics Ltd, Glasgow, Scotland, U.K., a company he co-founded in 2000. He is also with the University of Glasgow, Glasgow, Scotland, U.K., where he is Professor of Optoelectronic Systems in the Department of Electronics and Electrical Engineering. His research interests are concerned with linear and nonlinear integrated optoelectronic systems. He has developed new integration technologies for photonic integrated circuits based on quantum-well devices and intermixing, and has built up an extensive program of work at the University of Glasgow on III-V based photonic integrated circuits for high-speed digital optical communications. He is author or co-author of more than 300 journal and conference papers.

Dr. Marsh is a Fellow of the Institution of Electrical Engineers (IEE), the Royal Society of Arts (FRSA), and the Royal Society of Edinburgh (FRSE). He is a member of the IEEE Lasers and Electro-Optics Society (LEOS), the IEEE Electron Devices Society (EDS), the IEEE Communications Society, and the Optical Society of America. He is currently a member of the LEOS Optoelectronic Materials and Processing Technical Committee and of the EDS Optoelectronic Devices Technical Committee. From 1996 to 1998, he was Founding Chair of the Scottish Chapter of LEOS. From 1999 until 2001, he was LEOS Vice President of Membership and Regional Activities for Europe, the Middle-East, and Africa. He is an elected member of the LEOS Board of Governors (2001–2004), a member of the Executive Team of the IEE Photonics Network, a member of the Engineering and Physical Sciences Research Council's Electronic and Photonic Technologies College, and a member of the Council of the Scottish Optoelectronics Association.

C. J. Hamilton, photograph and biography not available at the time of publication.

C. C. Button, photograph and biography not available at the time of publication.